

# THE ROLE OF METAL ION ON PHYSIOCHEMICAL PROPERTIES OF METAL ALUMINATES PREPARED BY IMPREGNATION METHOD

S. Komeili<sup>1</sup>, M. Takht Ravanchi<sup>2</sup> and A. Taeb<sup>1</sup>

\* komeili@iust.ac.ir

Received: December 2016

Accepted: March 2017

<sup>1</sup> Chemical Engineering Department, Iran University of Science and Technology, Tehran, Iran.

<sup>2</sup> National Petrochemical Company, Petrochemical Research and Technology Company, Tehran, Iran.

**Abstract:** A series of  $MA_2O_4$  ( $M= Ni, Zn, \text{ and } Cu$ ) aluminates were prepared by using impregnation method; the metal content of the products was ranged between 5wt% to 25wt%. The samples were characterized by x-ray diffraction (XRD), Brunauer Emmett Teller (BET) surface area,  $NH_3$  temperature-programmed desorption ( $NH_3$ -TPD), and inductively coupled argon plasma (ICP).

The specific surface areas of zinc, nickel and copper aluminates were in the ranges of 47-77m<sup>2</sup>/g, 63-87m<sup>2</sup>/g and 1.6-3m<sup>2</sup>/g, respectively. The surface acidity decreased in the order of  $CuAl_2O_4 < NiAl_2O_4 < ZnAl_2O_4 < Al_2O_3$ . By increasing the amount of metals in the samples, the number of acidic sites decreased, but their strength did not significantly change. Ni-aluminates have fewer acidic sites than Zn-aluminates, particularly in strong acid sites.

**Keywords:** Aluminate, Impregnation, Acidity, Catalyst Support

## 1. INTRODUCTION

Metal aluminates have many different practical applications in the fields of engineering and chemistry, which includes; adsorbents, coatings, soft abrasives, pigments, fillers, sensors, magnetic materials, catalysts, and supporting materials for catalysts [1, 2]. Aluminates can be used as supporting materials for catalysts due to their chemical and physical stability, high mechanical resistance, hydrophobicity, and low surface acidity [1, 3- 5].

The preparation of metal aluminates is interesting in general and specifically with respect to the effect of the ionic metal on the aluminate properties. Abatzoglou et al. [6] synthesized Ni aluminates (5wt% Ni) by two methods including a wet impregnation on the  $\gamma$ - $Al_2O_3$  powder and coprecipitation. They calcined the samples at 900°C. A metastable nickel aluminate ( $NiAl_{10}O_{16}$ ) formed in both preparation methods. However, the impregnated catalyst had a second active spinel ' $NiAl_2O_4$ ' phase that grew at the expense of the metastable phase. The coprecipitation method provided a more homogeneous catalyst with higher surface area than the impregnation method. Ertel et al. [7] prepared nickel and copper aluminates by

impregnation and calcination at 800°C. The samples contained metal oxide crystals (CuO and NiO) by the surface area was in the range of 75-80m<sup>2</sup>/g. Sueiras et al. [8, 9] prepared Mg, Cu, and Zn aluminates by impregnation on various alumina, which included gibbsite, boehmite, and gamma and alpha alumina. They used calcination temperature in the range of 900-1100°C. The metal ions had some impacts on the formation rate of spinels and alumina phase transformation. They results showed that specific surface area of samples calcined at 1000°C were 46m<sup>2</sup>/g, 68m<sup>2</sup>/g, and 11m<sup>2</sup>/g for Zn, Mg, and Cu, respectively. Kiss et al. [5] investigated the influence of nickel loading (5, 10, and 20 wt% Ni), heat treatment temperature (400°C, 700°C, and 1100°C), and method of catalyst preparation (impregnation, mechanical powder mixed versus coprecipitation) on catalytic properties. Adanez et al. [10] prepared nickel aluminates (6-30wt% Ni) on gamma and alpha alumina by the impregnation method, calcined the samples at 950°C, and considered the resulting crystalline phases. The green NiO crystals detected in the samples prepared by  $\alpha$ - $Al_2O_3$  and the blue samples containing high fraction of  $NiAl_2O_4$  in the case of carriers prepared by  $\gamma$ - $Al_2O_3$ . Trawczynski et al. [11] used impregnation of

alumina with zinc salts, coprecipitation and hydrothermal synthesis to prepare zinc aluminates that calcined at 600°C.

Base of our knowledge, no report has been published to study and compare the role of Ni, Zn and Cu aluminates prepared with the same impregnation method by various amount of metals. In this work, nickel, zinc, and copper precursor liquids were impregnated on porous spherical  $\gamma$ -alumina. The samples were calcined at 1050°C to produce related aluminates with different metal contents. Structural, textural and acidity properties of products were investigated.

## 2. EXPERIMENTAL

### 2. 1. Materials

Commercial spherical  $\gamma$ -Al<sub>2</sub>O<sub>3</sub> (BET: 210.13 m<sup>2</sup>/g and pore volume: 0.53 cm<sup>3</sup>/g) was supplied from Sasol Co. The copper nitrate trihydrate (Cu(NO<sub>3</sub>)<sub>2</sub>.3H<sub>2</sub>O), Merck No.102753; nickel nitrate hexahydrate (Ni(NO<sub>3</sub>)<sub>2</sub>.6H<sub>2</sub>O), Merck No.105821; and zinc nitrate tetrahydrate (Zn(NO<sub>3</sub>)<sub>2</sub>.4H<sub>2</sub>O), Merck No. 108833 were used as metal precursors.

### 2. 2. Preparation

Nickel and zinc salt was melted on the heater, the melting point of hydrated zinc, nickel and copper nitrate is 45°C, 57°C, and 115°C, respectively. Desired amount of alumina placed in an oven at 120°C for 1h to remove physically adsorbed water and then placed in the oil bath at 110-120°C. The melted precursors were impregnated on the alumina for 30min in the oil bath. A series of samples were prepared in 0.2, 0.5, 0.8 mL/g, ratio of volume of metal (Ni, Zn, and Cu) precursor per weight of alumina. The samples were dried in the oven at 120°C for 16h and then stepwise were calcined in the electrical furnace by 1°C/min to 300°C and remained for 2h then by 3°C/min to 500°C for 1h and by 5°C/min to 1050°C for 3h. A  $\gamma$ -alumina was calcined in the same condition for comparison.

### 2. 3. Characterization

The X-ray diffraction (XRD) pattern of Al<sub>2</sub>O<sub>3</sub> supports was carried out using an X-ray diffractometer (Model GNRMPD 3000) with Cu-K $\alpha$  radiation at 40kV and 30mA.

The surface area was determined by N<sub>2</sub> physisorption using an adsorption analyser type Quantachrome Nova 2200. The BET measurements, nitrogen adsorption-desorption isotherms and pore structure analysis conducted at 77K. The pore size distribution was determined by the Barrett-Joyner-Halenda (BJH) method.

The water-displacement method was used for measuring the volume of macro pores [12]. For such study, dry samples were weighted and immersed in water at 70°C for 1h; then cooled to ambient temperature. The difference between the weight of a saturated sample in air and dry sample was set as the weight of water displacement in pores and by using water density, pore volume was calculated.

Temperature-programmed desorption (TPD) measurements of NH<sub>3</sub> were performed in BELCAT A. Ammonia adsorption was carried out at 60°C in a mixture of NH<sub>3</sub> (2.5cc/min) and He (47.5cc/min) flowed for 1h. The product was then exposed to helium for 30min at 60°C to remove all the physically adsorbed species before starting the temperature program. The samples adsorbed ammonia at 60°C heated up to 700°C with a heating rate of 10°C/min. The amount of acid sites on the catalyst surface was calculated based on desorption amount of ammonia. Desorption signals were monitored by a TCD detector.

The metal content of the samples was determined by inductively coupled plasma (ICP-OES simultaneous instrument, model: VISTA-PRO, Varain).

## 3. RESULTS AND DISCUSSION

### 3. 1. Metal Content

The amounts of nickel, zinc, and copper measured by the ICP technique are given in table 1. As expected, increasing the volume of

Table 1. Amount of metal in each sample measured by ICP

Sample name	Ni <sub>0.2</sub>	Ni <sub>0.5</sub>	Ni <sub>0.8</sub>	Zn <sub>0.2</sub>	Zn <sub>0.5</sub>	Zn <sub>0.8</sub>	Cu <sub>0.2</sub>	Cu <sub>0.5</sub>	Cu <sub>0.8</sub>
precursor/alumina (cm <sup>3</sup> /g)	0.2	0.5	0.8	0.2	0.5	0.8	0.2	0.5	0.8
Amount of metals(wt%)	Nickel			Zinc			Copper		
	11.05	15.70	24.86	5.50	12.61	16.14	9.94	16.47	20.19

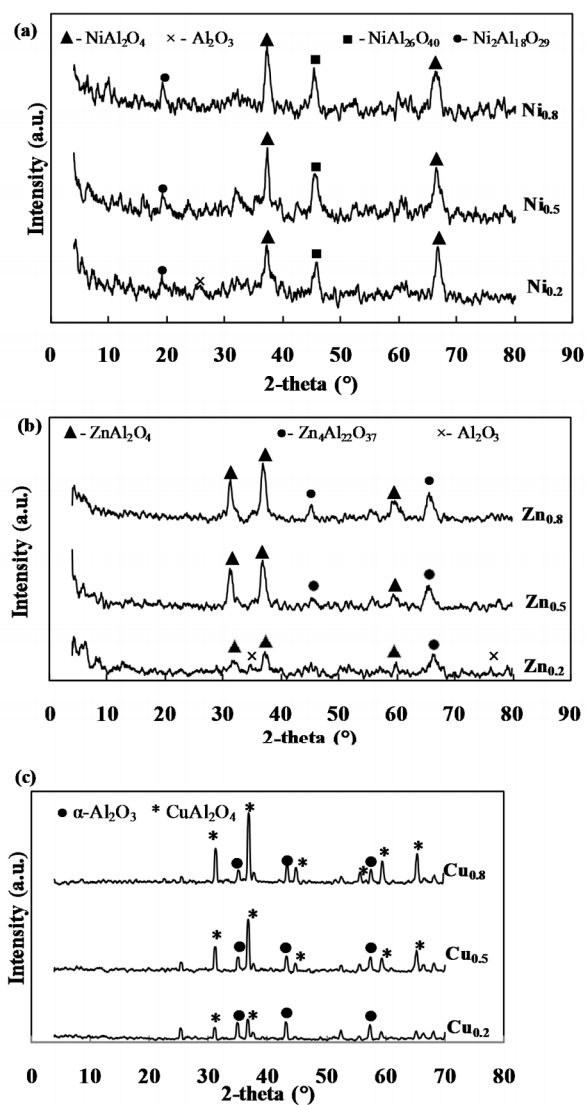


Fig. 1. XRD pattern of metal aluminates with various metal contents (a) nickel, (b) zinc and (c) copper

precursors in contact with the surface of alumina increased the amount of reachable metal, allowing more metal to enter the alumina structures during heat treatment. These findings confirmed that the prepared samples had different amounts of metal.

### 3. 2. Structures

The XRD patterns of Ni, Zn, and Cu modified  $\text{Al}_2\text{O}_3$  by various metal contents are shown in Fig. 1. Copper aluminate pattern was different in comparison with nickel or zinc aluminate. The XRD patterns of  $\text{CuAl}_2\text{O}_4$  (Fig. 1(c)) contain sharp peaks that indicate the samples have high crystallinity in comparison by zinc and nickel aluminates that have lower crystallinity, as indicated by the presence of more overlapping peaks in their XRD patterns. The presence of copper ions in the alumina structures accelerated the alumina transformation phase, as the XRD patterns only depict alpha alumina in these samples, while the zinc and nickel aluminate samples have amorphous alumina (Fig. 1a, b). Other studies confirmed that copper ions penetrated the alumina much deeper and faster than zinc or nickel ions [13, 14].

Increasing the metal content of the aluminates was led to enlargement, broadening, and intensifying the XRD peaks, indicating formation of a greater number of aluminate structures. The formation of spinels related to the local concentration of metals in the  $\text{Al}_2\text{O}_3$  matrix. Higher metal content may lead to higher spinel concentration during the impregnation process [6].

The monoclinic  $\text{Ni}_2\text{Al}_{18}\text{O}_{29}$  (ICDD No. 22-0451), tetragonal  $\text{NiAl}_{26}\text{O}_{40}$  (ICDD No. 20-0776), and cubic  $\text{NiAl}_2\text{O}_4$  (ICDD No. 10-0339) structures are indicated in Fig. 1(a). Two zinc aluminate structures,  $\text{ZnAl}_2\text{O}_4$  (ICDD No.5-0669) in cubic and  $\text{Zn}_4\text{Al}_{22}\text{O}_{37}$  (ICDD No.23-1491) in hexagonal structures, are shown in Fig. 1(b). These structures related to the concentration and distribution of cations; in general, the cation distribution showed the metal ions in the tetrahedral coordination and the aluminium ions in the octahedral coordination. At high temperatures, a random ordering occurred with

some metal ions changing to octahedral coordination and the Al ions changing from octahedral to tetrahedral coordination [3]. The largest peaks at  $37.2^\circ$  and  $66.3^\circ$  were for  $\text{NiAl}_2\text{O}_4$  and at  $31.2^\circ$  and  $36.8^\circ$  were for  $\text{ZnAl}_2\text{O}_4$  structures, confirming the samples contained high fraction of  $\text{NiAl}_2\text{O}_4$  and  $\text{ZnAl}_2\text{O}_4$ , respectively.

The patterns of the copper aluminates (Fig. 1(c)) coincided with the standard data of the cubic spinel Cu aluminate phase (ICDD-PDF No. 33-0448) and alpha alumina phase (ICDD-PDF: 46-1212). The mean crystal size of  $\text{CuAl}_2\text{O}_4$  was 34.5nm and of alpha alumina was in the range of 36.1-39.0nm; these were calculated using the Scherrer equation (Eq.1).

$$\tau = \frac{K\lambda}{\beta \cos \theta} \quad (1)$$

where K is a shape factor with a typical value of approximately 0.9,  $\lambda$  the X-ray wavelength equal to 1.54,  $\beta$  the line broadening at half of the maximum intensity (FWHM), and  $\theta$  the Bragg angle [15].

The alpha alumina detected in all copper samples was potentially explained by the action of  $\text{CuAl}_2\text{O}_4$  as a diffusion barrier that resulted in the major rate-limiting step enabling complete spinel transformation. The transformation rate lowered with thickening of the  $\text{CuAl}_2\text{O}_4$  zone, as it became more difficult for Al and Cu to counter-diffuse [14].

### 3. 3. Textures

The nitrogen adsorption-desorption isotherms and the pore size distribution plots of the nickel and zinc samples are shown in Figs. 2(a) and (b), respectively. The isotherm profiles of Ni and Zn are close to type IV according to the International Union of Pure and Applied Chemistry classification, indicating a mesoporous material. The copper aluminate samples show type II isotherms (Fig. 2(c)), which are characteristic of non-porous or macroporous materials [16].

As seen in Fig. 3(a), the pore size distribution

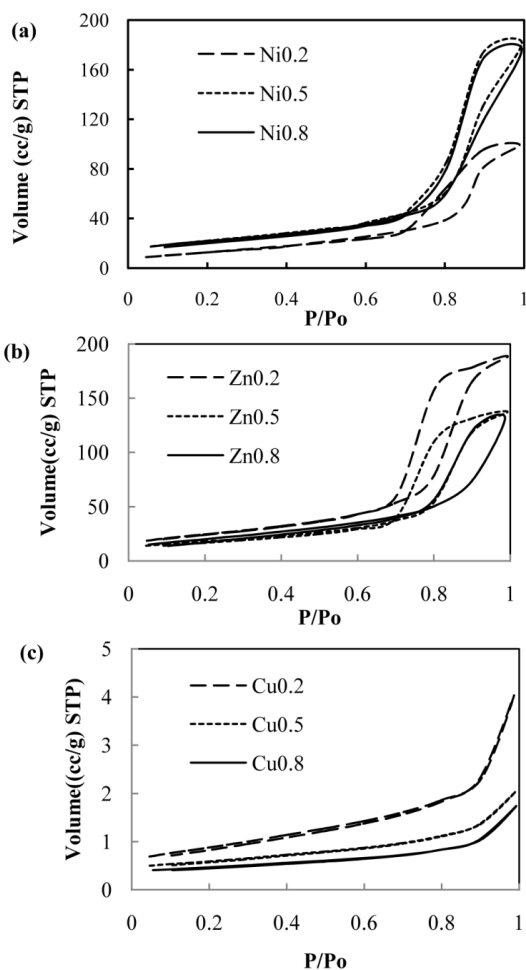


**Fig. 2.**  $N_2$  adsorption-desorption isotherms of (a) nickel, (b) zinc, and (c) copper aluminates

of  $Ni_{0.2}$  covered a large range (2-93nm), including mesopores and macropores, but the average pore diameter was 9nm, indicating that the material was predominantly mesoporous, which was further confirmed by the hysteresis loop in Fig. 2(a). The textural properties of  $Ni_{0.5}$  and  $Ni_{0.8}$  were almost similar. The average pore diameter was 15nm, with pore size distribution in the wide range of 2-180 nm for both of them. Fig. 3(b) shows the corresponding pore-size distribution curves of zinc aluminates.  $Zn_{0.2}$  and  $Zn_{0.5}$  displayed a rather narrow unimodal distribution in the range of 5-16nm; but the distribution was broader for  $Zn_{0.8}$ , including

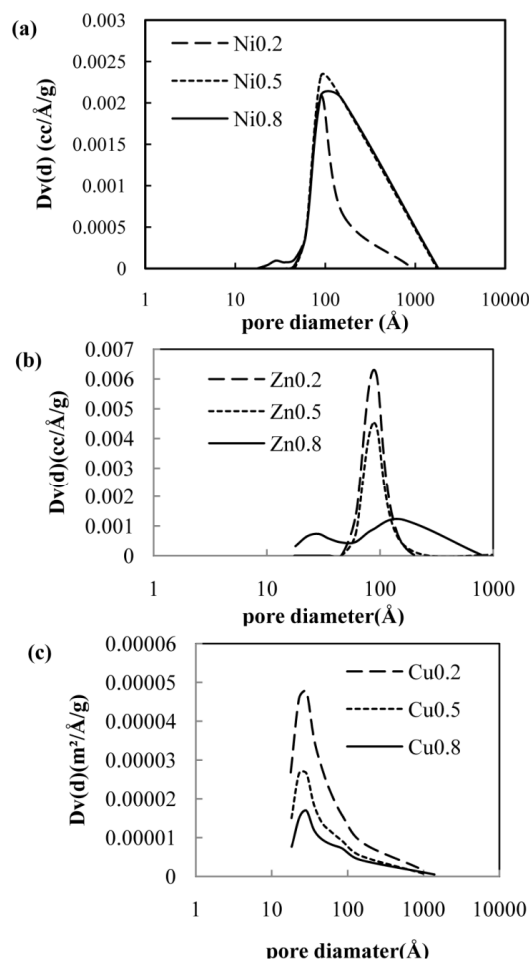


**Fig. 3.** Pore size distribution (a) nickel, (b) zinc and (c) copper aluminates

mesopores and macro pores (size range of 2-80 nm), with a mean pore diameter of 16 nm. Figure 3(c) shows the mesopore size distributions for the copper aluminates; the tails at the upper end of the distribution were at pore sizes larger than 100 nm. The vertical axis of Fig. 3(c) has the numbers, 2 or 3 orders lower than others. So the cu-aluminate products had a few amount of pores. Therefore, this figure shows very few pores had the radius around 10nm. These pores had not any effect to produce significant surface area Cu-contained samples. As the  $N_2$  isotherms confirmed, these samples were non-porous so the very low surface area were obtained.

**Table 2.** Textural properties of samples

Sample	Specific surface area (m <sup>2</sup> /g)	Pore volume (mL/g)	Pore diameter(nm)
Ni <sub>0.2</sub>	46.75	0.15	9
Ni <sub>0.5</sub>	78.33	0.29	15
Ni <sub>0.8</sub>	77.38	0.28	15
Zn <sub>0.2</sub>	87.54	0.31	9
Zn <sub>0.5</sub>	63.50	0.23	9
Zn <sub>0.8</sub>	72.83	0.21	16
Cu <sub>0.2</sub>	3.11	0.3*	437
Cu <sub>0.5</sub>	2.04	0.2*	451
Cu <sub>0.8</sub>	1.58	0.2*	481
*evaluated by water displacement			

**Table 3.** Amount of desorbed ammonia and maximum temperature of each peak from NH<sub>3</sub>-TPD

Sample	Peak No.	Max. peak temperature (°C)	Amount of ammonia (mmol/g)
Alumina (Ni <sub>0</sub> or Zn <sub>0</sub> )	1	149	0.151
	2	318	0.145
	3	523	0.403
Ni <sub>0.2</sub>	1	162	0.152
	2	293	0.080
	3	501	0.136
Ni <sub>0.5</sub>	1	151	0.193
	2	507	0.085
Ni <sub>0.8</sub>	1	142	0.204
	2	496	0.076
Zn <sub>0.2</sub>	1	148	0.220
	2	510	0.200
Zn <sub>0.5</sub>	1	164	0.206
	2	520	0.198
Zn <sub>0.8</sub>	1	156	0.146
	2	508	0.143
Cu <sub>0.2</sub>	-	-	0.023
Cu <sub>0.5</sub>	-	-	0.043
Cu <sub>0.8</sub>	-	-	0.063

Increasing the amount of zinc and copper in the samples caused the pore size distribution to become wider and smaller. Conversely, these variations were not present for the nickel aluminate samples. Zn and Cu ions had greater influence on porosity disturbance of the samples; this may be related to their structures.

The specific surface areas of  $\text{Ni}_{0.2}$ ,  $\text{Ni}_{0.5}$ , and  $\text{Ni}_{0.8}$  were 47, 78, and 77  $\text{m}^2/\text{g}$ , respectively (Table 2). These were high surface areas in comparison with those obtained by other researchers who prepared samples using solvothermal (10.5 to 14.9  $\text{m}^2/\text{g}$ ) and sol-gel (1.6 to 2.3  $\text{m}^2/\text{g}$ ) methods [2, 3, 17]. The textural properties of  $\text{Ni}_{0.5}$  and  $\text{Ni}_{0.8}$  are the same, and their specific pore volumes were 0.29  $\text{mL}/\text{g}$  and 0.28  $\text{mL}/\text{g}$ , respectively.

For the Zn aluminate samples, the specific surface area was in the range of 63-87  $\text{m}^2/\text{g}$ , with a mean pore diameter in the range of 9-16 nm and specific pore volume in the range of 0.2-0.3  $\text{mL}/\text{g}$ . The copper aluminates had a low surface area (1.6-3  $\text{m}^2/\text{g}$ ) with macroporous structures. The high crystallinity and low surface area of Cu samples showed that the impregnation method at the calcination temperature used in this study in the presence of Cu leads to a sintering effect that destroys the pores.

A subsequent study that used other preparation methods reported the formation of a new pure phase (such as copper aluminate and alpha alumina) that resulted in a low surface area with large pores. The copper aluminate sample prepared via the sol-gel route and calcined at 900°C had a surface area in the range of 10.3-41.8  $\text{m}^2/\text{g}$  [8, 18].

### 3. 4. Acidity

Surface acidity is one of the properties of interest of aluminates for catalytic applications. Fig. 4 shows the  $\text{NH}_3$ -TPD profiles of the nickel, zinc, and copper aluminates and alumina for comparison. Each peak corresponds to a different type of acid site. Usually, the first peak relates to a weak acid site, a moderate-temperature peak to a medium acid site, and a high-temperature peak to a strong acid site. The amount of desorbed ammonia related to each peak and the maximum

peak temperature are given in Table 3.

The peaks for all metal aluminates were quite small in comparison with those for alumina. For Ni-aluminates, the reduction in the number of moderate and strong acid sites was striking, with the peaks near 300°C and 500°C almost disappearing. Desorption peaks for strong and medium acid sites decreased rapidly and the profiles became almost flat as the amount of Ni increased, suggesting that the acidity of the alumina significantly decreased with the

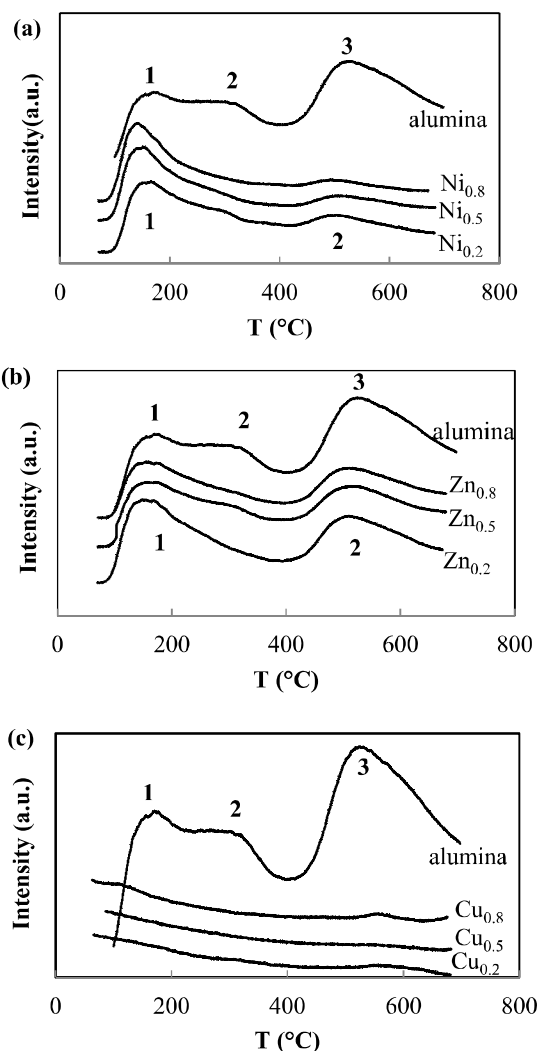


Fig.4. Desorption of ammonia as a function of temperature (a) nickel, (b) zinc and (c) copper aluminate sample

incorporation of Ni atoms and  $\text{NiAl}_2\text{O}_4$  formation (Fig. 4(a)) [2].

The Zn aluminate samples had lower acidity than alumina but higher total acidity sites than Ni aluminate, specifically with respect to the strong acid ( $T > 500^\circ\text{C}$ ) [17]. By increasing the metal content (Zn, Ni) in samples, larger amount of aluminates formed led to decrease in the total acid sites. This reduction of acid sites was more for Zn aluminate than for Ni aluminates. The ratio of weak per strong acid sites for Ni samples was around twice that of Zn samples. In another work, the Zn aluminates prepared by impregnation and calcined at  $600^\circ\text{C}$  had an acidity of approximately  $0.47\text{mmol/g}$ , where the atomic Al: Zn ratio equals two [11].

The graphs were almost flat for the copper aluminate samples (Fig. 4(c)). Table 3 shows the low level of ammonia adsorption; this finding was attributable to the low surface area of these aluminates.

By adding Ni or Zn to alumina, the strength of acid sites confirmed by maximum peak temperature dose not significantly change for weak acid sites; for strong acid sites, it slightly decreased.

The obvious differences existed in the surface acidity and textural properties of Ni, Zn, and Cu aluminates that were prepared by impregnation method. This finding encouraged us to the further study these materials as the catalyst support in a given process.

#### 4. CONCLUSION

The metal ions used for the creation of aluminates strongly influence their textural and acidic structure. Copper aluminates had the lowest porosity, with a large pore diameter (in the range expected for macropores) and high crystallinity. Conversely, nickel and zinc aluminates were mesoporous and have a higher surface area. Different aluminate structures existed among the samples considered in this study. Overall, the aluminate acidity trend was in the order of alumina > Zn-aluminate > Ni-aluminate >> Cu-aluminate.

#### 5. ACKNOWLEDGEMENTS

The authors gratefully acknowledge the financial support received in the form of a research grant (project No. 870249110) from the Petrochemical Research and Technology Company (NPC-RT), Iran.

#### REFERENCES

1. Deraz, N. M., "Synthesis and characterization of nano-sized nickel aluminate spinel crystals". *Int. J. Electrochem. Sci.*, 2013, 8, 5203-5212.
2. Mekasuwandumrong, O., Wongwaranon, N., Panpranot, J. and Praserttham, P., "Effect of Ni-modified  $\alpha\text{-Al}_2\text{O}_3$  prepared by sol-gel and solvothermal methods on the characteristics and catalytic properties of Pd/ $\alpha\text{-Al}_2\text{O}_3$  catalysts". *Mater. Chem. Phys.*, 2008, 111, 431-437.
3. Ribeiro, N. F. P., Neto, R. C. R., Moya, S. F., Souza, M. V. M. and Schmal, M., "Synthesis of  $\text{NiAl}_2\text{O}_4$  with high surface area as precursor of Ni nanoparticles for hydrogen production". *Int. J. Hydrogen Energ.*, 2010, 35, 11725-11732.
4. Zhou, L., Guo, Y., Zhang, Q., Yagi, M., Hatakeyama, J., Li, H., Chen, J., Sakurai, M. and Kameyama, H., "A novel catalyst with plate-type anodic alumina supports, Ni/ $\text{NiAl}_2\text{O}_4$ /  $\gamma\text{-Al}_2\text{O}_3$  / alloy for steam reforming of methane. *Appl. Catal. A Gen.*, 2008, 347, 200-207.
5. Kiss, E. E., Lazi, M. M. and Bošković, G. C., "Catalyst component interactions in nickel /alumina catalysts". *APTEFF*, 2007, 38, 61-68.
6. Achouri, E. I., Abatzoglou, N., Lefebvre, F. C. and Braidy, N., "Diesel steam reforming: Comparison of two nickel aluminate catalysts prepared by wet-impregnation and co-precipitation". *Catal. Today*, 2013, 207, 13-20.
7. Ertl, G., Hierl, R., Knozinger, H., Thiele, N. and Urbach, H. P., "XPS study of copper aluminate catalysts", *Appl. Surf. Sci.*, 1980, 5, 49-64.
8. Alexandre, A., Medina, F., Salagre, P., Fabregat, A. and Sueiras, J. E., "Characterization and activity of copper and nickel catalysts for the oxidation of phenol aqueous solutions". *Appl. Catal. B Environ.*, 1998, 18, 307-315.
9. Kiss, E., Ratkovic, S., Vujicic, D. and Boskovic, G., "Accelerated polymorphous transformations

- of alumina induced by copper ions impede spinel formation". *Indian J. Chem.*, 2012, 51, 1669-1676.
10. Adánez, J., Labiano, F. G., Diego, L. F., Gayán, P., Celaya, J. and Abad, A., "Nickel-Copper oxygen carriers to reach zero CO and H<sub>2</sub> emission in chemical-looping combustion", *Ind. Eng. Chem. Res.*, 2006, 45, 2617-2625.
  11. Trawczynski, J., Kubacki, A., Wrzyszczyk, J., Zawadzki, M., Grabowska, H. and Mista, W., "Zinc aluminates as supports for HDS catalysts", *React. Kinet. Catal. Lett.*, 2002, 76, 259-264.
  12. Manger, G. E., "Method-dependent values of bulk, grain, and pore volume as related to observed porosity", *Geological survey bulletin*, Washington, USA, 1966, 1-20.
  13. Bolt, P. H., Habraken, F. H. P. M. and Geus, J. W., "Formation of Nickel, Cobalt, Copper, and Iron Aluminates from  $\alpha$ - and  $\gamma$ -Alumina-Supported Oxides: A Comparative Study". *J. Solid State Chem.*, 1998, 135, 59-69.
  14. Hu, C. Y., Shih, K. and Leckie, J. O., "Formation of copper aluminate spinel and cuprous aluminate delafossite to thermally stabilize simulated copper-laden sludge". *J. Hazard. Mater.*, 2010, 181, 399-404.
  15. Takht Ravanchi, M., Rahimi Fard, M., Fadaee Rayeabi, S., Yaripour, F., "Effect of Calcination Conditions on Crystalline Structure and Pore Size Distribution for a Mesoporous Alumina". *Chem. Eng. Commun.*, 2015, 202, 493-499.
  16. Sing, K. S. W.; Everett, D. H., Haul, R. A. W., Moscou, L., Pierotti, R. A., Rouquerol, J. and Siemieniowska, T., "Reporting Physisorption data for gas/solid systems with Special Reference to the Determination of Surface Area and Porosity (IUPAC)". *Pure App. Chem.*, 1985, 57, 603-619.
  17. Chinayon, S., Mekasuwandumrong, O., Praserttham, P. and Panpranot, J., "Selective hydrogenation of acetylene over Pd catalysts supported on nanocrystalline  $\alpha$ -Al<sub>2</sub>O<sub>3</sub> and Zn-modified  $\alpha$ -Al<sub>2</sub>O<sub>3</sub>". *Catal. Commun.*, 2008, 9, 2297-2302.
  18. Kumar, T. R., Suresh, P., Selvam, C. S. N., Kennedy, J. L. and Vijaya, J., "Comparative study of nano copper aluminate spinel prepared by sol-gel and modified sol-gel techniques: Structural", electrical, optical and catalytic studies. *J. Alloy. Compound.*, 2012, 522, 39-45.